Thermal-magnetic-electric oscillator based on spin-valve effect

Kadigrobov, Anatoli; Andersson, Sebastian; Park, Hee Chul; Radić, Danko; Shekhter, Robert; Jonson, Mats; Korenivski, Vladislav

Source / Izvornik: **Journal of Applied Physics, 2012, 111**

Journal article, Published version
Rad u časopisu, Objavljena verzija rada (izdavačev PDF)

https://doi.org/10.1063/1.3686735

Permanent link / Trajna poveznica: https://urn.nsk.hr/urn:nbn:hr:217:112078

Thermal-magnetic-electric oscillator based on spin-valve effect

A. M. Kadigrobov, S. Andersson, Hee Chul Park, D. Radić, R. I. Shekhter et al.

Citation: J. Appl. Phys. **111**, 044315 (2012); doi: 10.1063/1.3686735
View online: http://dx.doi.org/10.1063/1.3686735
View Table of Contents: http://jap.aip.org/resource/1/JAPIAU/v111/i4
Published by the American Institute of Physics.

Thermal-magnetic-electric oscillator based on spin-valve effect

A. M. Kadigrobov,[1,2,a)] S. Andersson,[3] Hee Chul Park,[1,4] D. Radić,[1,5] R. I. Shekhter,[1] M. Jonson,[1,6,7] and V. Korenivski[3]
[1]*Department of Physics, University of Gothenburg, Göteborg SE-412 96, Sweden*
[2]*Theoretische Physik III, Ruhr-Universität Bochum, Bochum D-44801, Germany*
[3]*Nanostructure Physics, Royal Institute of Technology, Stockholm SE-106 91, Sweden*
[4]*Department of Physics, Chungnam National University, Daejeon 305-764, South Korea*
[5]*Department of Physics, Faculty of Science, University of Zagreb, Zagreb 1001, Croatia*
[6]*School of Engineering and Physical Sciences, Heriot-Watt University, Edinburgh EH14 4AS, Scotland, United Kingdom*
[7]*Division of Quantum Phases and Devices, School of Physics, Konkuk University, Seoul 143-701, South Korea*

(Received 4 February 2011; accepted 24 January 2012; published online 24 February 2012)

A thermal-magnetic-electric valve with the free layer of exchange-spring type and inverse magnetoresistance is investigated. The structure has S-shaped current-voltage characteristics and can exhibit spontaneous oscillations when integrated with a conventional capacitor within a resonator circuit. The frequency of the oscillations can be controlled from essentially dc to the GHz range by the circuit capacitance. © *2012 American Institute of Physics*. [doi:10.1063/1.3686735]

I. INTRODUCTION

Electrons in ferromagnetic conductors are differentiated with respect to their spin due to the exchange interaction, which leads to a splitting of the corresponding energy bands and to a non-vanishing polarization of the conduction electrons. This spin polarization gives rise to a number of "spintronic" effects in magnetic nanostructures, such as giant magnetoresistance (GMR)[1,2] and spin-transfer-torque.[3,4]

A conventional GMR spin valve has low resistance in the parallel configuration of the two ferromagnetic layers and high resistance in the antiparallel configuration. The GMR is said to be inverse when the low resistance state corresponds to the antiparallel orientation of the ferromagnets.[5] Inverse GMR is observed in, for example, spin valves incorporating minority carrier ferromagnetic layers.[6–9] Another possible implementation of the inverse GMR spin-valve, demonstrated in this paper, relies on an antiparallel exchange-pinning of two ferromagnetic layers of different coercivity to two antiferromagnetic layers.

We have previously analyzed a novel spin-thermo-electronic (STE) oscillator[10] based on a GMR exchange-spring multilayer[11] having an N-shaped current-voltage characteristic (IVC) connected in series to an inductor (L), which performs the function of current limiting in the circuit and thereby determines its oscillation frequency. A tunable inductor, such as the one having a magnetic core,[12,13] can be used to achieve a tunable oscillator. However, in applications where the device footprint is tightly budgeted, it may be advantageous to employ a mirror-circuit configuration. Namely, an inverse GMR spin valve with an S-shaped IVC connected to a capacitor (C) in parallel. This paper provides a detailed analysis of this new structure as well as a comparison of the two STE oscillator designs. We show that the STE-C design proposed herein offers an attractive, compact alternative to the STE-L oscillator discussed previously.[10]

II. S-SHAPED CURRENT-VOLTAGE CHARACTERISTIC UNDER JOULE HEATING: CONTROL OF THE MAGNETIZATION DIRECTION BY DC BIAS CURRENT

We consider a system of three ferromagnetic layers in which two strongly ferromagnetic layers 0 and 2 are exchange coupled through a weakly ferromagnetic spacer (layer 1), while layer 3 is ferromagnetic and separated from layer 2 by a potential barrier that interrupts their exchange interaction; the magnetoresistance of the stack is normal, being mainly determined by the magnetization direction of layer 2 with respect to the one of layer 3, as illustrated in Fig. 1. We assume that the Curie temperature, $T_c^{(1)}$, of layer 1 is lower than the Curie temperatures, $T_c^{(0,2,3)}$, of layers 0, 2 and 3. We also assume the magnetization direction of layers 0 and 3 to be fixed and antiparallel; layer 2 is subject to a magnetic field, H, directed opposite to the magnetization of layer 0, which can be an external field, the fringing field from layer 0, or a combination of the two. We require this magneto-static field to be weak enough so that, at low temperatures, T, the magnetization of layer 2 is kept parallel to the magnetization of layer 0 due to the exchange interaction between them via layer 1. In the absence of the external field, and if the temperature is above the Curie point of the spacer, $T > T_c^{(1)}$, this tri-layer is similar to the spin-flop "free layer" widely used in memory device applications.[14]

As it was shown in Ref. 10, parallel orientations of the magnetization in layers 0, 1, and 2 become unstable if the

a)Author to whom correspondence should be addressed. Electronic addresses: anatoli.kadygrobov@physics.gu.se and kadig@tp3.rub.de.

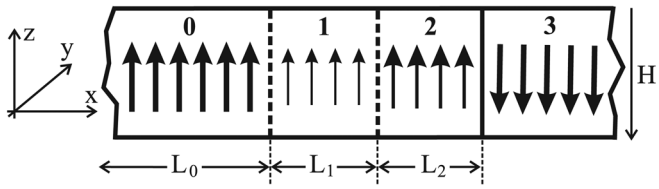

FIG. 1. Orientation of the magnetic moments in a stack of 4 layers (0, 1, 2, 3), in which the magnetic moments in layers 0, 1, and 2 are coupled by the exchange interaction, thus building an exchange spring tri-layer; H is an external magnetic field directed antiparallel to the magnetization in layer 0; layer 3 is a ferromagnetic separated from layer 2 by a potential barrier that interrupts their exchange interaction, the magnetization directions of layers 0 and 3 being fixed and antiparallel; the magnetoresistance of the stack is normal, being mainly determined by the magnetization direction of layer 2 with respect to the one of layer 3.

temperature exceeds some critical temperature, $T_c^{(\mathrm{or})} < T_c^{(1)}$. The magnetization direction in layer 2 tilts with an increase of the stack temperature, T, in the temperature range, $T_c^{(\mathrm{or})} \le T \le T_c^{(1)}$. The dependence of the equilibrium tilt angle, Θ, between the magnetization directions of layers 0 and 2 on T and the magnetic field, H, is determined by the equation[10]

$$\begin{aligned} \Theta = D(H, T)\sin\Theta, \quad & T < T_c^{(1)} \\ \Theta = \pm\pi, \quad & T \ge T_c^{(1)} \end{aligned}, \tag{1}$$

where

$$D(H, T) = \frac{L_1 L_2 H M_2(T)}{4\alpha_1 M_1^2(T)} \approx D_0(H)\frac{T_c^{(1)}}{T_c^{(1)} - T}, \tag{2}$$

$$D_0(H) = \frac{\mu_B H}{k_B T_c^{(1)}}\left(\frac{L_1}{a}\right)\left(\frac{L_2}{a}\right). \tag{3}$$

Here, L_1, $M_1(T)$ and L_2, $M_2(T)$ are the widths and the magnetic moments of layers 1 and 2, respectively; $\alpha_1 \sim J_1/aM_1^2(0)$ is the exchange constant, J_1 is the exchange energy in layer 1, μ_B is the Bohr magneton, k_B is the Boltzmann's constant, and a is the lattice spacing. Taking experimental values (see Ref. 10) $L_1 = 30$ nm, $L_2 = 12$ nm, $T_c^{(1)} = 373$K, and magnetic field $H = 10 \div 47$ Oe, one finds $D_0 = 0.1 \div 0.36$ and the temperature interval $T_c^{(1)} - T_c^{(or)} = D_0 T_c^{(1)} \approx 37.3 \div 134$ K. The parameter $D(H, T)$ is the ratio between the magnetic energy and the energy of the stack volume for the inhomogeneous distribution of the magnetization. At low temperatures, the exchange energy prevails, the parameter $D(H, T) < 1$, and Eq. (1) has only one root, $\Theta = 0$; thus, a parallel orientation of magnetic moments in layers 0, 1, and 2 of the stack is thermodynamically stable. However, at temperature, $T_c^{(\mathrm{or})} < T_c^{(1)}$, for which

$$D(T_c^{(\mathrm{or})}, H) = 1,$$

two new solutions, $\Theta = \pm|\theta_{\min}| \neq 0$, appear. The parallel magnetization corresponding to $\Theta = 0$ is now unstable, and the direction of the magnetization in region 2 tilts with an increase of temperature inside the interval, $T_c^{(\mathrm{or})} \le T \le T_c^{(1)}$. For the case $D_0 \ll 1$, according to Eq. (2), the critical temperature, $T_c^{(\mathrm{or})}$, of this orientational phase transition (The orientational phase transition in such a system induced by an external magnetic field was considered in Ref. 15) is equal to

$$T_c^{(\mathrm{or})} = T_c^{(1)}\left(1 - \frac{\delta T}{T_c^{(1)}}\right), \quad \frac{\delta T}{T_c^{(1)}} = D_0(H). \tag{4}$$

If the stack is Joule heated by current, I, its temperature, $T(V)$, is determined by the heat-balance condition

$$IV = Q(T), \quad I = V/R(\Theta) \tag{5}$$

and Eq. (1), which determines the temperature dependence of $\Theta[T(V)]$. Here, V is the voltage drop across the stack, $Q(T)$ is the heat flux from the stack, and $R(\Theta)$ is the total stack magnetoresistance. Here and below, we neglect the dependence of the magnetoresistance on T, because we consider the case that variations of the temperature caused by the Joule heating takes place in a narrow vicinity of $T_c^{(1)}$, which is sufficiently lower than the critical temperatures $T_c^{(0,2)}$.

Equations (5) and (1) define the IVC of the stack

$$I_0(V) = \frac{V}{R[\Theta(V)]}, \tag{6}$$

where $\Theta(V) \equiv \Theta[T(V)]$.

The differential conductance of the stack[10] is

$$\frac{dI_0}{dV} = R(\Theta)\left.\frac{[R^{-1}(\Theta)(1 - \bar{D}\sin\Theta/\Theta)]'}{[R(\Theta)(1 - \bar{D}\sin\Theta/\Theta)]'}\right|_{\Theta=\Theta(V)}, \tag{7}$$

where $[\ldots]'$ means the derivative of the bracketed quantity with respect to Θ and

$$\bar{D} = \left.\frac{T}{Q}\frac{dQ}{dT}D_0\right|_{T=T_c^{(1)}} \approx D_0.$$

As follows from Eq. (7), the current-voltage characteristic, $I_0(V)$, may be N- or S-shaped, depending on whether the magnetoresistance of the stack increases or decreases with an increase of the angle, Θ. In the case that the stack has a normal magnetoresistance (that is, $dR/d\Theta > 0$), the IVC is N-shaped, so nonlinear current and magnetization-direction oscillations may spontaneously arise if the stack is incorporated in a voltage-biased electrical circuit in series with an inductor.[10] In this paper, we consider the situation in which $dR/d\Theta < 0$. This condition is obtained if the stack has its configuration (Condition $dR/d\Theta < 0$, which is necessary to obtain an S-shaped IVC, can be also obtained in the case where layer 3 is nonmagnetic, but the magnetoresistance of layers 0 and 2 is inverse shown in Fig. 1). One can readily see that the magnetoresistance of such a stack is maximal at $\Theta = 0$.

As one can see from Eq. (7), if $dR/d\Theta < 0$, the numerator of the differential conductance is always positive, while the denominator can be negative and, hence, the IVC of the stack is S-shaped, as illustrated in Fig. 2. For the magnetoresistance of the stack in the form

$$R(\Theta) = R_+(1 + r\cos\Theta), \tag{8}$$

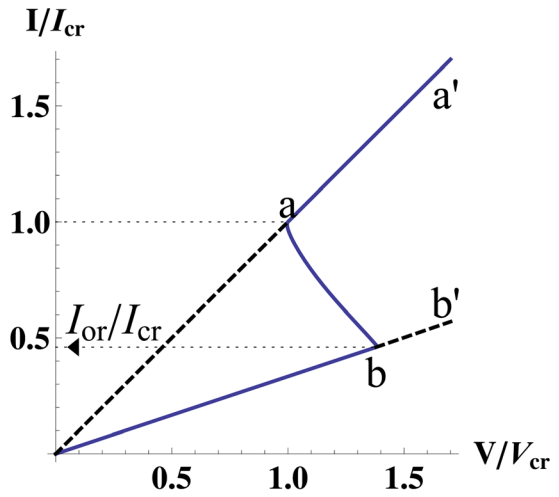

FIG. 2. (Color online) Current-voltage characteristics (IVC) of the magnetic stack from Fig. 1 calculated for $R(\Theta) = R_+(1 + r\cos\Theta)$, $R(\pi)/R(0) = 0.3$, $\bar{D} = 0.36$, $I_{cr} = \sqrt{Q(T_c^{(1)})/R(\pi)}$, and $I_{or} = \sqrt{Q(T_c^{(or)})/R(0)}$. Branches $0 - b$ and $a - a'$ of the IVC correspond to parallel and antiparallel orientations of the magnetization of layers 0 and 2, respectively (parts $0 - a'$ and $b - b$ are unstable); branch $a - b$ corresponds to the tilt of the magnetization of layer 2 with respect to that of layer 0 (that is, $\Theta \neq 0$).

where

$$R_+ = \frac{R(0) + R(\pi)}{2}; \qquad r = \frac{R(0) - R(\pi)}{R(0) + R(\pi)} > 0, \tag{9}$$

one finds that the differential conductance $dI_0/dV < 0$ if

$$\bar{D} < \frac{3r}{1 + 4r}. \tag{10}$$

While writing Eqs. (8)–(10), we have neglected the explicit temperature dependence of the magnetoresistance, as it is weak[16,17] as compared with the temperature dependence which arises via the angle $\Theta(T)$ determined by Eq. (1). If one takes into account the explicit temperature dependence of the magnetoresistance, $R = R(T, \Theta)$, one finds that the differential conductance is negative if

$$\left.\frac{d(R(T, \Theta[T])Q(T))}{dT}\right|_{T=T(V)} < 0,$$

where the bias voltage dependence of the temperature, $T = T(V)$, is determined by Eq. (5) together with Eq. (1).

We note here that the modulus of the negative differential conductance may be large, even in the case that the magnetoresistance is small. Using Eq. (7) at $r \ll 1$, one finds the differential conductance, G_{diff}, as

$$G_{diff} \equiv \frac{dJ}{dV} = -R^{-1}(0)\frac{1 + \bar{D}/3r}{1 - \bar{D}/3r}, \tag{11}$$

which is negative provided $3r > \bar{D}$, the modulus of G_{diff} being of the order of $R^{-1}(0)$; the widths of the section of the IVC with the negative differential conductance on the current and voltage axes are $\delta V \approx rV$ and $\delta j \approx rj$, respectively.

Therefore, if $r \ll 1$, the minimal possible magnetoresistance factor for observation of the negative differential resistance is limited either by the precision of the electrical measurements δj_m and δV_m in the experiment, $r > \delta j_m/j$, $\delta V_m/V$, or by the geometrical factor of the stack $r > D_0$ (see Eq. (3)). Alternatively, one may say that the size of the stack is limited by the inequality

$$\left(\frac{L_1}{a}\right)\left(\frac{L_2}{a}\right) < 3r\frac{k_B T_c^{(1)}}{\mu_B H}. \tag{12}$$

Here and below, we consider the case that the electric current flowing through the sample is lower than the torque critical current and, hence, the torque effect is absent.[18–20]

In Sec. III, we show that, in the case of the S-shaped IVC, $I_0(V)$, current and magnetization oscillations arise if the stack is incorporated in a current-biased circuit in parallel with a capacitor. In this case, the thermo-electronic control of the relative orientation of layers 0 and 2 may be of two types, depending on the ratio between the resistance of the stack, $R(\Theta)$, and the resistance of the rest of the circuit, $R_{\rm rst}$.

As one can see from Fig. 2, if the bias current I_{bias} through the stack is controllably applied (that is, $R_{\rm rst} \gg R(\Theta)$), the voltage drop across the stack is uniquely determined from the IVC, $I_{bias} = I_0(V)$, and, hence, the relative orientation of the magnetization of layers 0 and 2 (that is, the tilt angle, Θ) can be changed smoothly from parallel ($\Theta = 0$) to anti-parallel $\Theta = \pi$ by varying the bias current through the interval $I_{or} \leq I_{\rm bias} \leq I_{cr}$. This corresponds to moving along the $a - b$ branch of the IVC. The dependence of the magnetization direction, Θ, on the current flowing through the stack is shown in Fig. 3.

In the voltage-bias regime, on the other hand, where the resistance of the stack is much larger than the resistance of the rest of the circuit, $R(\Theta) \gg R_{\rm rst}$, the voltage across the stack V is kept at a given value approximately equal to the bias voltage. Since the IVC is S-shaped, the stack can now be in a bistable state: in the voltage range between points a and b, there are three possible values of the current for one fixed value of voltage (see Fig. 2). The states of the stack with the lowest and the highest currents are stable, while the state of the stack with the middle value of the current is

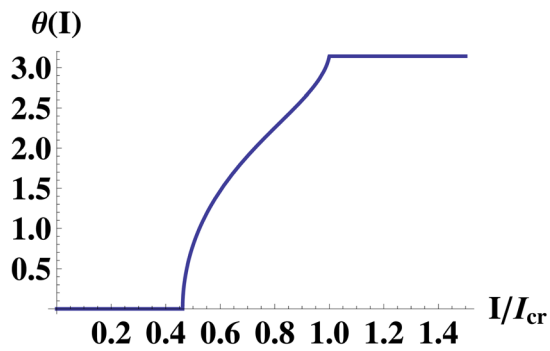

FIG. 3. (Color online) The angle Θ, which describes the tilt of the direction of the magnetization in layer 2 with respect to layer 0 as a function of the current in the current-biased regime. The curve was calculated for $R(\Theta) = R_+(1 + r\cos\Theta)$, $R(\pi)/R(0) = 0.3$, $\bar{D} = 0.36$, and $I_{cr} = \sqrt{Q(T_c^{(1)})/R(0)}$.

unstable. Therefore, a change of the voltage results in a hysteresis loop: an increase of the voltage along the $0-b$ branch of the IVC leaves the magnetization directions in the stack parallel $(\Theta = 0)$ up to point b, where the current jumps to the upper branch $a-a'$, the jump being accompanied by a fast switching of the stack magnetization from the parallel $(\Theta = 0)$ to the antiparallel orientation $(\Theta = \pi)$. A decrease of the voltage along the $a'-a$ IVC branch keeps the stack magnetization antiparallel up to point a, where the current jumps to the lower $0-b$ branch of the IVC and the magnetization of the stack returns to the parallel orientation $(\Theta = 0)$.

In Sec. III, we show that, if the stack is connected in parallel with a capacitor and the capacitance exceeds some critical value, the above time-independent state becomes unstable and spontaneous temporal oscillations appear in the values of the current, voltage across the stack, temperature, and direction of the magnetization.

III. SELF-EXCITED ELECTRICAL, THERMAL, AND DIRECTIONAL MAGNETIC OSCILLATIONS

A. Current perpendicular to layer planes (CPP)

We consider now a situation where the magnetic stack under investigation is incorporated into an electrical circuit in parallel with a capacitor of capacitance, C, and the circuit is biased by a DC current, $I_{\rm bias}$, illustrated by the equivalent circuit of Fig. 4. The thermal and electrical processes in this system are governed by the set of equations

$$\begin{aligned} C_V \frac{dT}{dt} + Q(T) - R^{-1}(\Theta)V^2 = 0, \\ C\frac{dV}{dt} + R^{-1}(\Theta)V = I_{\rm bias}, \end{aligned} \tag{13}$$

where C_V is the heat capacity. The relaxation of the magnetic moment to its thermodynamic equilibrium direction is assumed to be the fastest process in the problem, which implies that the magnetization direction corresponds to the equilibrium state of the stack at the given temperature $T(t)$. In other words, the tilt angle $\Theta = \Theta(T(t))$ adiabatically

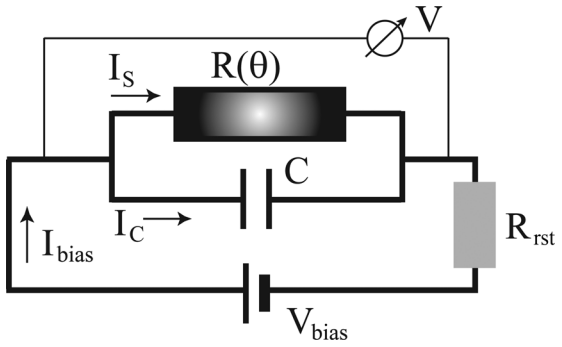

FIG. 4. Equivalent circuit for a Joule-heated magnetic stack of the type shown in Fig. 1. A resistance, $R[\Theta(t)] = I(t)/V(t)$, biased by a fixed DC current, $I_{\rm bias}$, is connected in parallel with a capacitor C; $R(\Theta)$ and $R_{\rm rst}$ are the angle-dependent resistance of the stack and the resistance of the rest of the circuit, respectively; $I(\Theta)$ and I_c are the currents flowing through the stack and the capacitor, respectively.

follows the time-evolution of the temperature and, hence, its temperature dependence is given by Eq. (1).

A time-dependent variation of the temperature is accompanied by a variation of the tilt angle $\Theta(T(t))$ and, hence, by a change in the voltage via the dependence of the magnetoresistance on this angle, $R = R(\Theta)$.

The system of equations in Eq. (13) has one time-independent solution $(\bar{T}(I_{bias}),\ \bar{V}(I_{bias}))$, which is determined by the equations

$$R^{-1}[\Theta(T)]\,V^2 = Q(T), \quad R^{-1}[\Theta(T)]\,V = I_{bias}. \tag{14}$$

This solution is identical to the solution of Eqs. (1) and (5) that determines the S-shaped IVC shown in Fig. 2 with a change $I \to I_{bias}$ and $V \to \bar{V}$.

In order to investigate the stability of this time-independent solution, we write the temperature, current, and angle as a sum of two terms:

$$\begin{aligned} T &= \bar{T}(I_{bias}) + T_1(t); \\ V &= \bar{V}(I_{bias}) + V_1(t); \\ \Theta &= \bar{\Theta}(I_{bias}) + \Theta_1(t), \end{aligned} \tag{15}$$

where T_1, V_1, and Θ_1 are small corrections. Inserting Eq. (15) into Eq. (13) and Eq. (1), one easily finds that the time-independent solution in Eq. (14) is always stable at any value of the capacitance C if the bias current I_{bias} corresponds to a branch of the IVC with a positive differential resistance (branches a–a′ and 0–b in Fig. 2). If the bias current I_{bias} corresponds to the branch with a negative differential resistance ($I_{or} < I_{bias} < I_{cr}$; see Fig. 2), the solution of the set of linearized equations is $T_1 = T_1^{(0)}\exp\{\gamma t\}$, $V_1 = V_1^{(0)}\exp\{\gamma t\}$, and $\Theta_1 = \Theta_1^{(0)}\exp\{\gamma t\}$, where $T_1^{(0)}$, $V_1^{(0)}$, and $\Theta_1^{(0)}$ are any initial values close to the time-independent state of the system and

$$\gamma = \frac{1}{2\bar{R}C}\left(\frac{C - C_{cr}}{C_{cr}} \pm \sqrt{\left(\frac{C - C_{cr}}{C_{cr}}\right)^2 - 4\frac{\bar{R}}{|R_d|}\frac{C}{C_{cr}}}\right), \tag{16}$$

where

$$C_{cr} = \left.\frac{C_V}{|d(RQ)/dT|}\right|_{T=T(I_{bias})} \tag{17}$$

and $R_d = dV/dI$ is the differential resistance, $\bar{R} = R(\bar{\Theta})$.

As one can see from Eq. (16), the time-independent state in Eq. (14) loses its stability if the capacitance exceeds the critical value C_{cr}: that is, $C > C_{cr}$. In this case, a limit cycle appears in plane (V,T) (see, e.g., Ref. 21), associated with the arising self-excited, non-linear, periodic oscillations in temperature, $T = T(t)$, and voltage, $V = V\ (t)$. These are accompanied by oscillations of the current through the stack, $I_s(t) = V(t)/R[\Theta(t)]$, and of the magnetization direction $\Theta(t) = \Theta(T(t))$. In the case when $(C - C_{cr})/C_{cr} \ll 1$, the system undergoes nearly harmonic oscillations around the steady state (see Eq. (15)) with frequency $\omega = {\rm Im}\,[\gamma(C = C_{cr})]$. Therefore, the temperature, T, the voltage drop across the stack, V, the current through the stack, $I_s(t)$, and the magnetization direction, Θ, perform a periodic motion with frequency

$$\omega = \frac{1}{C_{cr}\sqrt{\bar{R}|R_d|}}. \tag{18}$$

With a further increase of the capacitance, the size of the limit cycle grows, the amplitude of the oscillations increases, and the oscillations become anharmonic, with their period decreasing with increasing capacitance.

In order to investigate the time evolution of the voltage drop and the current through the stack in more detail, it is convenient to change variables $(V(t), T(t))$ to $(V(t), \tilde{I}(t))$ and introduce auxiliary current $\tilde{I}(t)$ and voltage $V_0(t)$, related to each other through Eqs. (5) and (1). Thus, we define

$$\tilde{I}(t) = \sqrt{\frac{Q(T(t))}{R(T(t))}}, \quad V_0 = \tilde{I}(t)R(T(t)), \tag{19}$$

where $R(T) = R(\Theta(T))$. Comparing these expressions with Eq. (5) shows that, at any moment t, Eq. (19) gives the stationary IVC of the stack, $V_0 = V_0(\tilde{I})$, which is an inverse function of the current-voltage characteristic, $I_0(V)$, defined by Eq. (6) and shown in Fig. 2.

Differentiating $\tilde{I}(t)$ with respect to t and using Eqs. (13) and (19), one finds that the dynamic evolution of the system is governed by

$$\begin{aligned} \tau_0 \frac{d\tilde{I}}{dt} - \frac{V^2 - V_0^2(\tilde{I})}{2V_0(\tilde{I})} &= 0, \\ C\frac{dV}{dt} + \frac{\tilde{I}}{V_0(\tilde{I})}V &= I_{\text{bias}}, \end{aligned} \tag{20}$$

where

$$\tau_0 = \frac{C_V}{d(QR^{-1})/dT}\Big|_{T=T(\tilde{V})}.$$

Equation (19) indicates that, at any moment, t, the current through the stack, $I_s(t) = V(t)/R(T(t))$, is coupled with the auxiliary voltage, $\tilde{V}(t)$, by the following relation:

$$I_s = \frac{V}{V_0(\tilde{V})}\tilde{I}.$$

The coupled equations in Eq. (20) have only one time-independent solution: $V = V_0(I_{bias})$, where $V_0(I)$ is the voltage-current characteristic (its inverse function, $I_0(V)$, is shown in Fig. 2). However, in the interval $I_{or} \le I_{\text{bias}} \le I_{cr}$, this solution is unstable with respect to small perturbations if $C > C_{\text{cr}}$. As a result, periodic oscillations of $I(t)$ and $\tilde{V}(t)$ appear spontaneously, with $I(t)$, $\tilde{V}(t)$ moving along a limit cycle. The limit cycle in the I-V plane is shown in Fig. 5.

Eq. (1) and Eq. (19) show that the magnetization direction, $\Theta(t) = \Theta(T(t))$, and the stack temperature $T = T(t)$ follow these electrical oscillations adiabatically according to the relation

$$Q[T(t)] = \tilde{I}(t)V_0[\tilde{I}(t)].$$

Temporal oscillations of $\Theta(t)$ are shown in Fig. 6.

According to Eq. (20), the ratio between the characteristic evolution times of the voltage, $V(t)$, and current, $\tilde{I}(t)$, increases with an increase of the capacitance, resulting in a qualitative change of the character of oscillations in the limit, $C \gg C_{cr}$. In this case, the current and the voltage slowly move along branches $a - a'$ and $0 - b$ of the IVC (see Fig. 2)) at the rate $\dot{V}/V \approx 1/R_+C$ (here, $\dot{V} = dV/dt$), quickly switching between these branches at points a and b at the rate of $\sim R_+/\tau_0$ (see Fig. 7). Therefore, the stack in this limit periodically switches between the parallel and antiparallel magnetic states, as shown in Fig. 8.

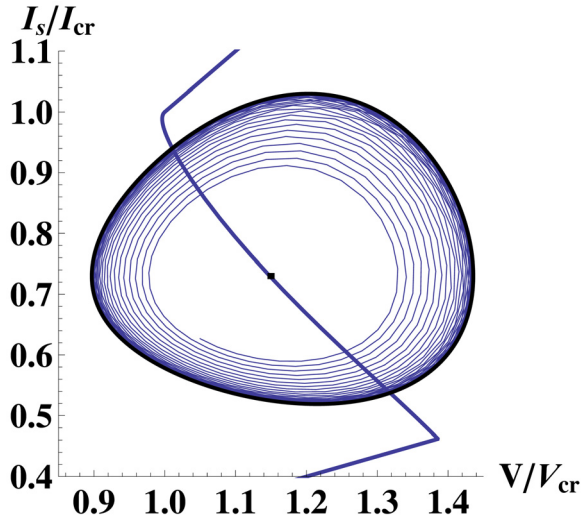

FIG. 5. (Color online) Spontaneous oscillations of the current through the stack, $I_s(t)$, and the voltage drop across it, $V(t)$, calculated for $R(\pi)/R(0) = 0.3$, $\bar{D} = 0.36$, and $(C - C_{\text{cr}})/C_{\text{cr}} = 0.062$; $I_{cr} = \sqrt{Q(T_c^{(1)})/R(\pi)}$ and $V_{cr} = R(\pi)I_{cr}$. $I_s(t)$ and $V(t)$ develop from the initial state toward the limiting cycle shown by the thick solid line, along which they execute a periodic motion. The stationary IVC of the stack is shown by the thin solid line.

B. Current in the layer planes (CIP)

If the electric current flows in the plane of the layers (CIP) of the stack, the torque effect is insufficient or absent,[3,20] while the magneto-thermal-electric oscillations under consideration may take place. In this case, the total current flowing through the cross-section of the layers may be presented as

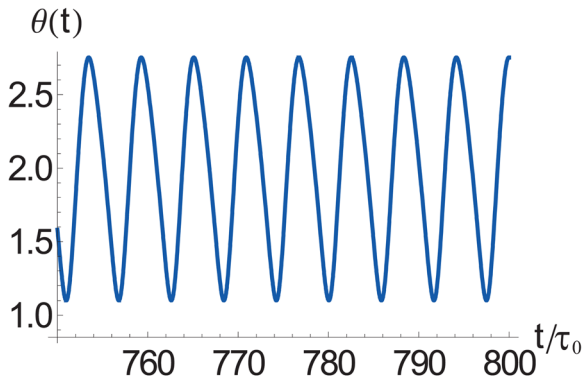

FIG. 6. (Color online) Spontaneous oscillations of the magnetization direction angle, $\Theta(t)$, associated with the periodic motion of $I_s(t)$ and $V(t)$ along the limiting cycle shown in Fig. 5; τ_0 is the characteristic evolution time of the current $\tilde{I}(t)$. Calculations are made for $R(\pi)/R(0) = 0.3$, $\bar{D} = 0.36$, and $(C - C_{\text{cr}})/C_{\text{cr}} = 0.062$.

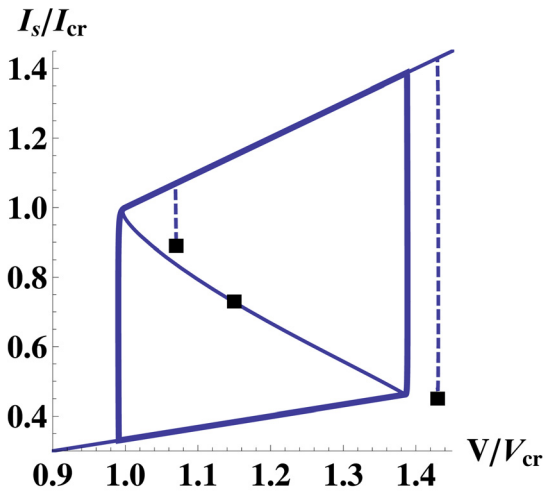

FIG. 7. (Color online) Spontaneous oscillations of current through the stack, $I_s(t)$, and voltage, $V(t)$, calculated for $R(\pi)/R(0) = 0.3$, $\bar{D} = 0.36$, and $C/C_{cr} = 520.91$. $I(t)$ and $V(t)$ develop toward the limit cycle (thick solid line) from the initial state, which can be either inside or outside it, and execute a periodic motion along the limit cycle. The stationary IVC of the stack is shown as a thin solid line.

$$J_{CIP} = \left(R^{-1}(\Theta) + R_0^{-1}\right) V, \tag{21}$$

where $R(\Theta)$ and R_0 are the magneto-resistance and the angle-independent resistance of the stack in the CIP set of the experiment.

In a CIP configuration, the stack is Joule heated by both the angle-dependent and the angle-independent currents and, hence, Eq. (5) should be re-written as follows:

$$J_{CIP}V = Q(T), \quad J_{CIP} = V/R_{CIP}(\Theta), \tag{22}$$

where

$$R_{CIP}(\Theta) = \frac{R(\Theta)R_0}{R(\Theta) + R_0}. \tag{23}$$

Using Eq. (7) and Eq. (21), one finds that the presence of the angle-independent current in the stack modifies the condition of the negative differential conductance $R_d^{(CIP)} = dJ_{CIP}/dV$: it is negative if

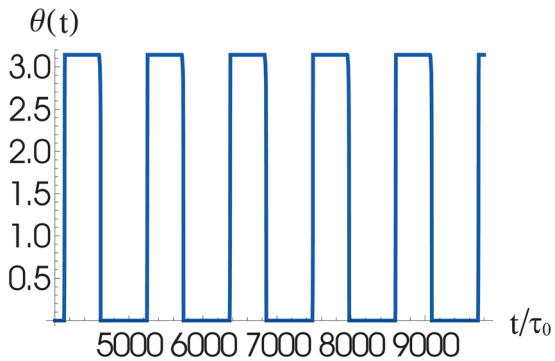

FIG. 8. (Color online) Spontaneous oscillations of the magnetization direction angle, $\Theta(t)$, associated with the periodic motion of $I_s(t)$ and $V(t)$ along the limiting cycle shown in Fig. 7; τ_0 is the characteristic evolution time of the current $\tilde{I}(t)$. Calculations are made for $R(\pi)/R(0) = 0.3$, $\bar{D} = 0.36$, and $C/C_{cr} = 520.91$.

$$\bar{D} < \frac{3rR_0}{(1+4r)R_0 + (1+r)^2 R_+}. \tag{24}$$

The time evolution of the system is described by the set of equations in Eq. (13), in which one needs to change $J \to J_{CIP}$ and $R(\Theta) \to R_{eff}(\Theta)$. Therefore, under this change, the temporal evolution of the system in a CIP configuration is the same as when the current flows perpendicular to the stack layers: if the bias voltage corresponds to the negative differential conductance $dJ_{CIP}/dV < 0$ and the capacitance exceeds the critical value

$$C_{cr} = \left.\frac{C_V}{|d(R_{CIP}Q)/dT|}\right|_{T=T(I_{bias})}, \tag{25}$$

self-excited oscillations of the current through the stack, J_{CIV}, voltage drop over it, V, and the temperature, T, and the angle, $\Theta(T(V))$, arise in the system, the maximal frequency of which being

$$\omega = \left.\frac{1}{C_{cr}\sqrt{R_{CIP}[\theta(I)]|R_d^{(CIP)}|}}\right|_{I=I_{bias}}. \tag{26}$$

Below, we present estimations of the critical inductance and the oscillation frequency, which are valid for both the above-mentioned CPP and CIP configurations of the experiment.

Using Eq. (14), one can estimate the order of magnitude of the critical capacitance C_{cr}, Eq. (17), and the oscillation frequency ω, Eq. (18), as $C_{cr} \approx Tc_v d/(\rho j)^2$ and $\omega \approx \rho j^2/Tc_v$, where c_v is the heat capacity per unit volume, ρ is the resistivity, and d is the characteristic size of the stack. For point contact devices with typical values of $d \sim 10^{-6} \div 10^{-5}$cm, $c_v \sim 1$ J/cm^{3}K, $\rho \sim 10^{-5}$ Ωcm, $j \sim 10^8$ A/cm^2, and, assuming that cooling of the device can provide the sample temperature $T \approx T_c^{(1)} \sim 10^2$K, one finds for the characteristic values of the critical capacitance and the oscillation frequency $C_{cr} \approx 10^{-11} \div 10^{-10}$F and $\omega \approx 1$GHz, respectively.

IV. FABRICATION OF THE SYSTEM WITH INVERSE GIANT MAGNETORESISTANCE

We will now show how the material system discussed above, with inverse GMR, can be fabricated using differential exchange-biasing. A schematic of the layer structure is shown in Fig. 9(a). The two ferromagnetic layers of the spin-valve (FM 1 and FM 2), each exchange pinned by an antiferromagnet (AFM 1 and AFM 2), are separated by a non-magnetic metal spacer (NM). Normally, the exchange-biasing procedure performed at a high field results in the two ferromagnets being pinned with their magnetization parallel to each other. In order to demonstrate inverse magnetoresistance, the exchange pinning must be altered such that the magnetization of the two ferromagnets become antiparallel. This can be done in two ways.

First, the blocking temperature of the two antiferromagnetic layers can be designed in fabrication such that one is lower than the other, $T_{B1} < T_{B2}$ or $T_{B2} < T_{B1}$.[22] By heating the sample to a temperature above the lower blocking temperature T_{B1} (T_{B2}), but below the higher blocking temperature T_{B2}

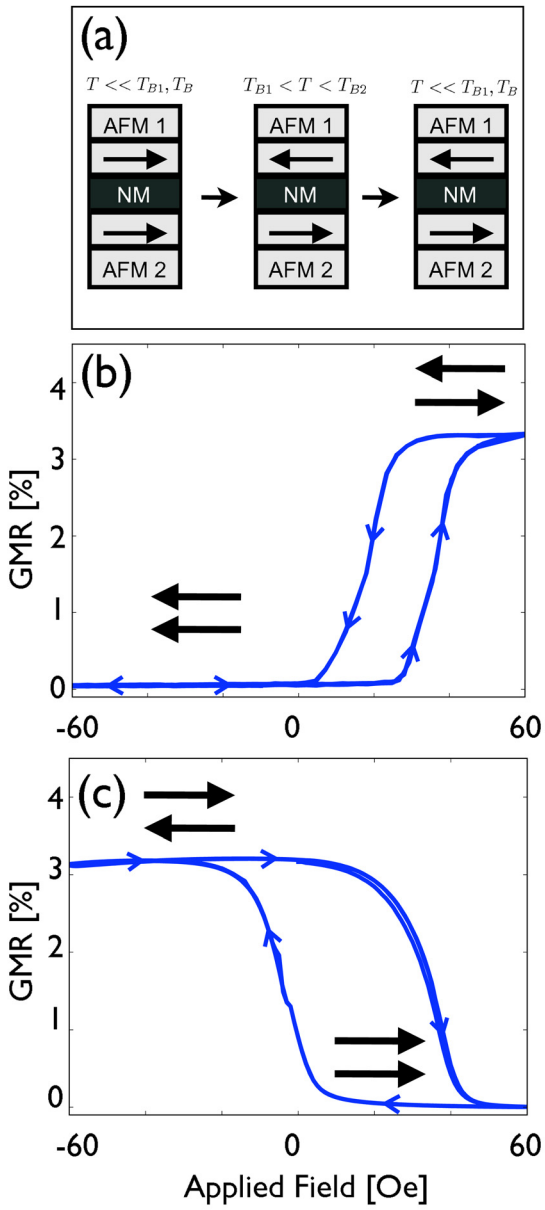

FIG. 9. (Color online) (a) Schematic of the studied material system: two ferromagnets, FM 1 and FM 2, each exchange pinned by an antiferromagnet, AFM 1 and AFM 2, are separated by a non-magnetic alloy, NM. The middle and right panels illustrate two methods to alter the exchange pinning such that the magnetization of the two ferromagnets become antiparallel. T_B is the antiferro-antiferromagnetic blocking temperature and H_C is the coercive field of the ferromagnets. (b) and (c) are minor magnetoresistance loops before and after the field-heat treatment, respectively. Arrows indicate the magnetization direction in FM 1 and FM 2.

(T_{B1}), the magnetization of FM 1 (FM 2) can be rotated by applying an external field. With FM 1 and FM 2 now antiparallel, the sample is cooled down to room temperature and the two ferromagnetic layers are pinned in opposition.

Second, one can use ferromagnets with different coercivity, $H_{C1} \neq H_{C2}$, and heat the sample to a temperature above both T_{B1} and T_{B2}. At this temperature, the ferromagnet with lower coercivity, FM 1 (FM 2), can be rotated in an external field if $H_{C1} < H_A < H_{C2}$ ($H_{C2} < H_A < H_{C1}$), where H_A is the applied field. With FM 1 and FM 2 now antiparallel, the sample is cooled down to room temperature. A schematic of these two methods are shown in Fig. 9(a). Below, we demonstrate the second method for obtaining an inverse GMR spin-valve using a practical material stack.

A series of films were deposited on thermally oxidized Si substrates using magnetron sputtering at a base pressure better than 5×10^{-8} Torr. Fifteen-nm-thick IrMn is used for AFM 1 and AFM 2. FM 1 is a thin bilayer of CoFe/NiFe and FM 2 is made up of CoFe/NiCu/CoFe/NiFe/CoFe, such that the two layers have different coercivity ($H_{C1} > H_{C2}$). To induce exchange coupling at the AFM/FM interfaces, the deposition was carried out in a magnetic field higher than 350 Oe. The complete structure of the sample was NiFe 3/IrMn 15/CoFe 2/NiCu 30/CoFe 2/NiFe 6/CoFe 4/Cu 7/CoFe 5/NiFe 3/IrMn 15/Ta 5, with the thicknesses in nanometers.

Using a vibrating sample magnetometer (VSM) equipped with an oven, the magnetization and switching fields of FM 1 and FM 2 could be monitored while the temperature was increased. At 180 °C, the temperature was higher than both T_{B1} and T_{B2}, which made it possible to align FM 1 and FM 2 antiparallel (since $H_{C1} > H_{C2}$). The external magnetic field was then removed and the sample was cooled down to room temperature. The minor magnetoresistance loop (current in plane magnetoresistance versus applied field when only the magnetization of FM 2 is switched) before and after the above field-heat treatment is shown in Fig. 9(b). It can be seen that, before the heat treatment, the resistance increases when a positive field of 30 Oe is applied. The same measurement for the same sample, but after the heat treatment, is shown in Fig. 9(c). The magnetoresistance has now become inverse, which means that the resistance decreases when a positive field is applied. The coercivity of FM 2 chosen for this demonstration of differential exchange pinning has increased somewhat as a result of the field-heat treatment. This issue should yield to optimization of the material stack and working with smaller blocking temperatures.

As regards to the size of the integrated oscillator, let us assume the typical resistance of the STE valve to be 50 Ω and the operating frequency ω = 1 GHz and estimate the required inductance L and capacitance C of the circuit. Thus, ωL = 50 Ω yields $L \sim 10^{-7}$ H, while $1/(\omega C)$ = 50 Ω yields $C \sim 10^{-11}$ F. The typical inductance of an on-chip inductor is 1 nH per mm of the wire length, somewhat enhanced if the wire is turned into a spiral. Therefore, the required chip area would be millimeters squared in size. A square parallel plate capacitor estimated using the standard formula for a typical dielectric material of a few-nm-thick insulator would measure 10 μm on the side. Obviously, a 100 000-fold reduction in the typical footprint should be achievable, in principle, by employing a device based on an S-shaped STE valve. In systems where tunability and high power are desirable, the N-shaped inductor based design may be preferable.

V. CONCLUSION

We have shown that Joule heating of an exchange-spring nanopillar with an inverse magneto-resistance results in a mutual coupling of the current and orientation of the switching layer. This allows us to control the magnetic alignment in the stack in the full range of angles from parallel to

antiparallel by varying the current through the structure. We have determined the range of parameters in which the current-voltage characteristic of the exchange-spring nanopillar with inverse magneto-resistance is S-shaped and evaluated a spin-thermionic oscillator, whose frequency can be varied by changing the capacitance in the circuit from essentially dc to the GHz range. A suitable material stack and method to produce the required inverse GMR spin valve is demonstrated.

ACKNOWLEDGMENTS

Financial support from the European Commission (FP7-ICT-FET Project No. 225955 STELE), the Swedish VR, and the Korean WCU program funded by MEST/NFR (R31-2008-00010057-0) is gratefully acknowledged.

[1]G. Binasch, P. Grünberg, F. Saurenbach, and W. Zinn, Phys. Rev. B **39**, 4828 (1989).
[2]M. N. Baibich, J. M. Broto, A. Fert, F. Nguyen Va Dau, and F. Petroff, Phys. Rev. Lett. **61**, 2472 (1988).
[3]J. C. Slonczewski, J. Magn. Magn. Mater. **159**, L1 (1996); **195**, L261 (1999).
[4]L. Berger, Phys. Rev. B **54**, 9353 (1996).
[5]C. Vouille, A. Barthélémy, F. Elokan Mpondo, A. Fert, P. A. Schroeder, S. Y. Hsu, A. Reilly, and R. Lolee, Phys. Rev. B **60**, 6710 (1999).
[6]J. M. George, L. G. Peraira, A. Barthélémy, F. Petroff, L. B. Steren, J. L. Duvail, A. Fert, R. Loloee, P. Holody, and P. A. Schroeder, Phys. Rev. Lett. **72**, 408 (1994).
[7]J. P. Renard, P. Bruno, R. Megy, B. Bbartenlian, P. Beauvillain, C. Chappert, C. Dupas, E. Kolb, M. Mulloy, P. Veillet, and E. Velu, Phys. Rev. B **51**, 12821 (1995).
[8]S. Y. Hsu, A. Barthélémy, P. Holody, R. Lolee, P. A. Schroeder, and A. Fert, Phys. Rev. Lett. **78**, 2652 (1997).
[9]C. Vouille, A. Fert, A. Barthélémy, S. Y. Hsu, R. Loloee, and P. A. Schroeder, J. Appl. Phys. **81**, 4573 (1997).
[10]A. M. Kadigrobov, S. Andersson, D. Radić, R. I. Shekhter, M. Jonson, and V. Korenivski, J. Appl. Phys. **107**, 123706 (2010).
[11]J. E. Davies, O. Hellwig, E. E. Fullerton, J. S. Jiang, S. D. Bader, G. T. Zimanyi, and K. Liu, Appl. Phys. Lett. **86**, 262503 (2005).
[12]V. Korenivski and R. B. van Dover, J. Appl. Phys. **82**, 5247 (1997).
[13]V. Korenivski, J. Magn. Magn. Mater., **215-216,** 800 (2000).
[14]V. Korenivski and D. C. Worledge, Appl. Phys. Lett. **86**, 252506 (2005).
[15]G. Asti, M. Solzi, M. Ghidni, and F. M. Neri, Phys. Rev. B **69**, 174401 (2004)
[16]For spin valves and MTJs, the T-dependence is typically less than a factor of 2 from 4 K to RT. Let us say from 30% at 4 K to 20% RT. So, 1% per 30 K or 0.03% per 1 K. We can say that "our own data" at near-above RT show similar small T-dependence.[17] It is important to note that, here and below, we consider variations of the temperature in the vicinity of the Curie temperature $T_c^{(1)}$ of the spacer, which is not in contact with the read-out spin-valve, while the Curie temperature $T_c^{(0)}$ of layer 2 is $T_c^{(0)} \gg T_c^{(1)}$.
[17]S. Andersson and V. Korenivski, IEEE Trans. Magn. **46**, 2140 (2010).
[18]Typical densities of critical currents needed for the torque effect in point-contact devices are $10^8 \div 10^9$ A/cm^2 for the current perpendicular to the layers (CPP). The record low torque critical current in a nanopillar device was reported in Ref. 19. (see Ref. 20). In our paper, we consider the case in which the torque effect is absent: that is, the torque critical current is higher than 10^8 A/cm^2.
[19]Z. Diao, Z. Li, S. Wang, Y. Ding, A. Panchula, E. Chen, L.-C. Wang, and Y. Huai, J. Phys.: Condens. Matter **19**, 165209 (2007).
[20]D. C. Ralph and M. D. Stiles, J. Magn. Magn. Mater. **320**, 1190 (2008).
[21]A. A. Andronov, A. A. Witt, and S. E. Khaikin, *Theory of Oscillations* (Pergamon, Oxford, 1966).
[22]I. L. Prejbeanu, W. Kula, K. Ounadjela, R. C. Sousa, O. Redon, B. Dieny, and J. P. Nozieres, IEEE Trans. Magn. **40**(4), 2625 (2004).